Supporting Information

Constructing phosphorus-doped TiO_2 hierarchical nanotube array via a simple route for the enhanced photoelectrochemical water oxidation

Xuejiao Ma, Qiusheng Wang, Jian Zhao*

[a] Tianjin Key Laboratory of Organic Solar Cells and Photochemical Conversion, School of Chemistry and Chemical Engineering, Tianjin University of Technology, Tianjin 300384, China.

*Email: zjtjbd@hotmail.com; zjtjbd@email.tjut.edu.cn

Table S1. Preparation of 0.2 M phosphate buffer at 25 °C.

pH	Volume of 0.2 M K_2HPO_4 (mL)	Volume of 0.2 M KH_2PO_4 (mL)
5.8	8.5	91.5
6.0	13.2	86.8
6.2	19.2	80.8
6.4	27.8	72.2
6.6	38.1	61.9
6.8	49.7	50.3
7.0	61.5	38.5
7.2	71.7	28.3
7.4	80.2	19.8
7.6	86.6	13.4
7.8	90.8	9.2
8.0	94.0	6.0
9.0	100.0	0.0

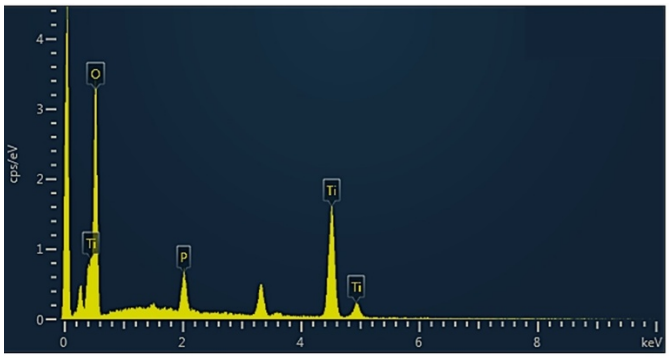

Figure S1. The EDS mapping analysis of P-TiO_2 HNTAs.

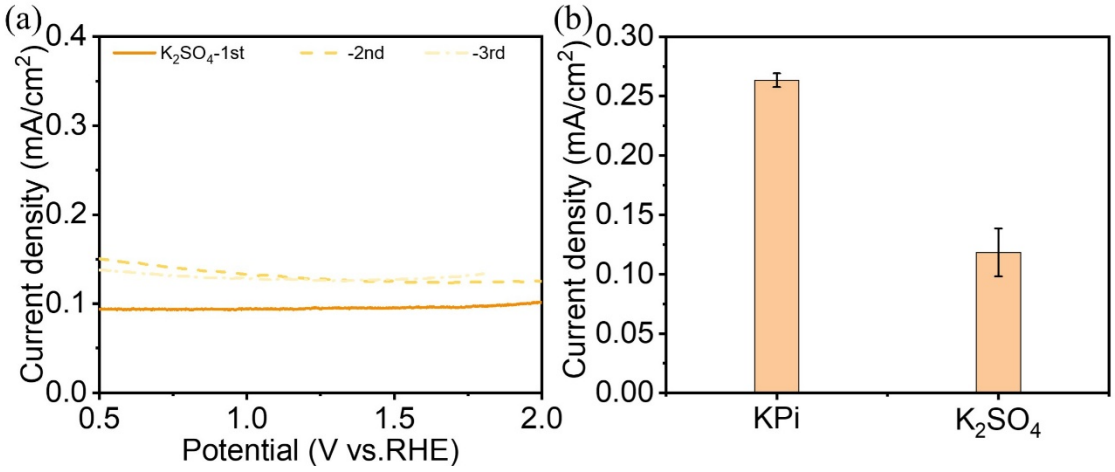

Figure S2. (a) The PEC water oxidation activity (LSV curve) of K-doped TiO_2 HNTAs obtained by immersing in K_2SO_4 instead of KPi, (b) The comparison of current density at 1.23 V vs. RHE with error bars for TiO_2 HNTAs obtained by immersing in K_2SO_4 and KPi as precursor. The error bar was obtained by repeating the experiment for three times (1^{st}, 2^{nd}, 3^{rd}). [Reaction condition: 0.5 M $NaSO_4$, Xenon lamp (AM 1.5G, 150 mW/cm^2), scan rate 20 mV/s.]

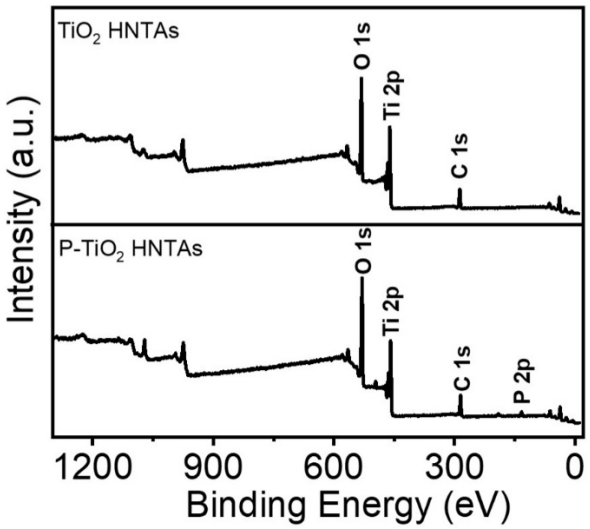

Figure S3. The full XPS spectrum of P-TiO_2 HNTAs.

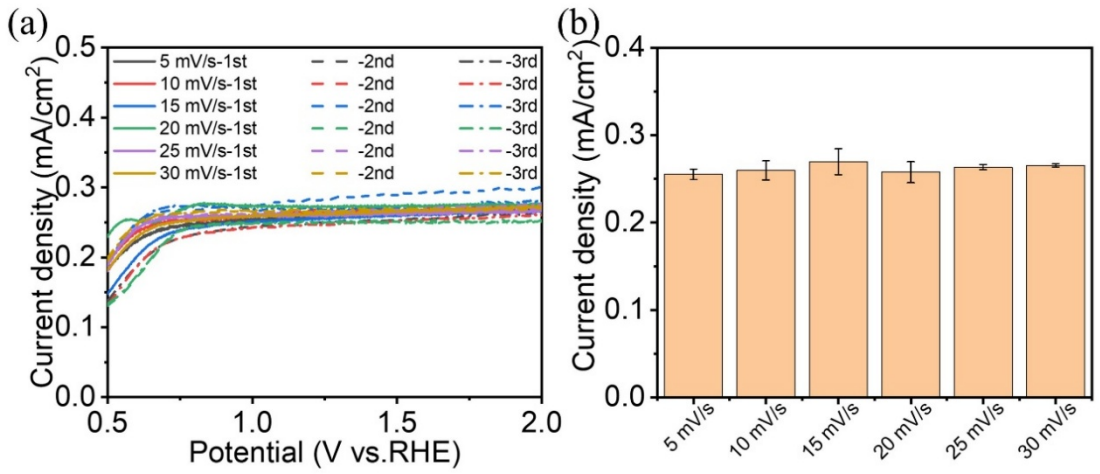

Figure S4. (a) The influence of scanning rate on the PEC water oxidation activity (LSV curves) of P-TiO_2 HNTAs. (b) The corresponding current density at 1.23 V vs. RHE. The error bars were obtained by repeating the experiment three times. [Reaction conditions: 0.5 M Na_2SO_4, Xenon lamp (AM 1.5G, 150 mW/cm^2).]

The scanning rate may lead to a significant overestimation of the photocurrent due to the charging current of the capacitor and the non-steady-state behavior. Therefore, to verify the optimized scan rate, we firstly conducted LSV tests at scanning rates of 5 mV/s, 10 mV/s, 15 mV/s, 20 mV/s, 25 mV/s, and 30 mV/s, respectively. As shown in Figure S4, as the scanning rate increases, the current density increases slightly, within the error range. Thus, a scan rate of 20 mV/s was chosen for the following investigation.

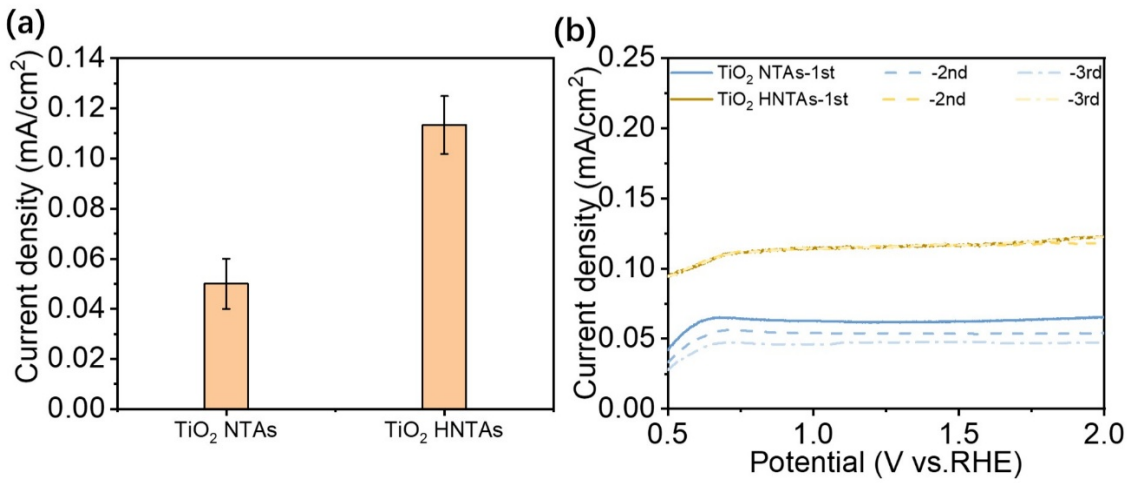

Figure S5. The performance of TiO_2 NTAs and TiO_2 HNTAs for PEC water oxidation. (a) The LSV curves and (b) corresponding current density at 1.23 V vs. RHE with error bars, obtained by repeating the experiments for three times (1^{st}, 2^{nd}, 3^{rd}). [Reaction condition: 0.5 M $NaSO_4$, Xenon lamp (AM 1.5G, 150 mW/cm^2), scan rate 20 mV/s.]

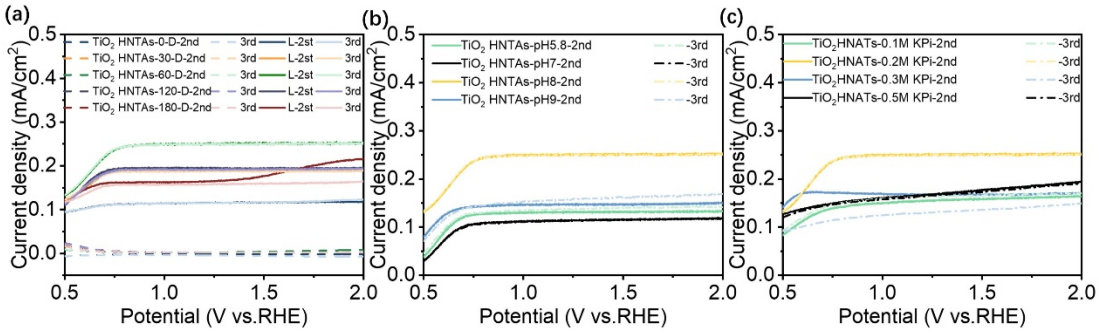

Figure S6. The PEC water oxidation activity (LSV curves) of TiO_2 HNTAs and P-doping TiO_2 HNTAs samples obtained via (a) different impregnation times, (b) pH and (c) concentration of KPi precursor, repeating the experiment for the 2nd and 3rd times. [Reaction condition: 0.5 M $NaSO_4$, Xenon lamp (AM 1.5G, 150 mW/cm^2), scan rate 20 mV/s.]

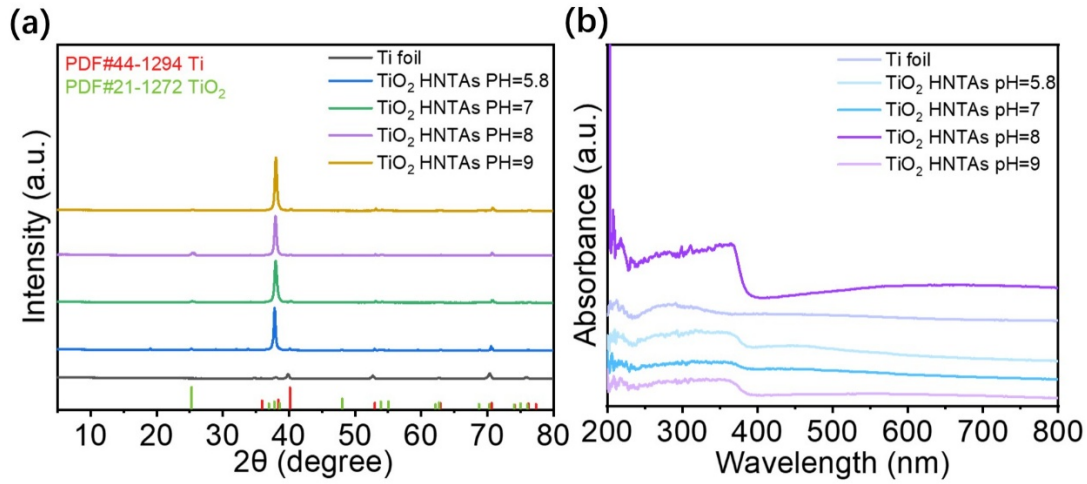

Figure S7. The (a) XRD and (b) UV-Vis absorption spectra of P-doping TiO_2 HNTAs samples prepared at different pH of KPi precursor.

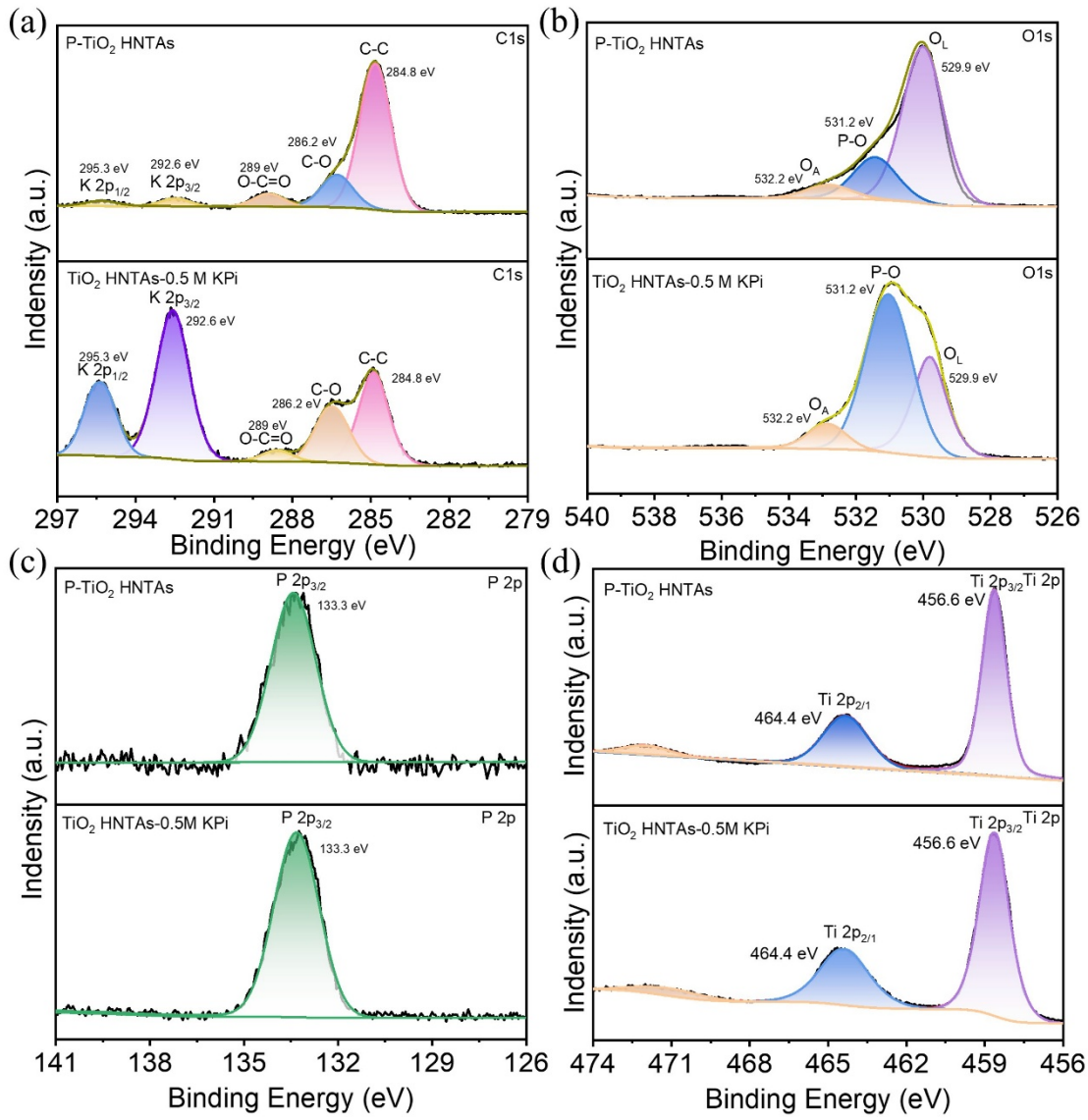

Figure S8. The comparison of XPS analysis for P-TiO_2 HNTAs and the sample dipped in high concentration KPi (TiO_2 HNTAs-0.5 M KPi). (a) O 1s, (b) Ti 2p (c) P 2p and (d) C 1s.

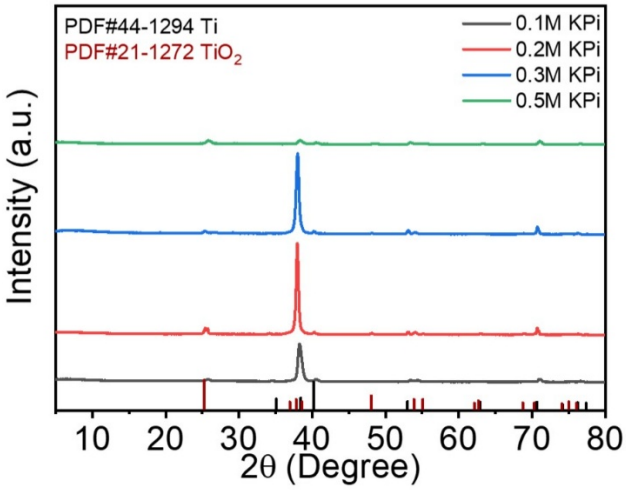

Figure S9. The XRD patterns of the P-doping TiO_2 HNTAs samples prepared by dipping in different concentration of KPi precursor.

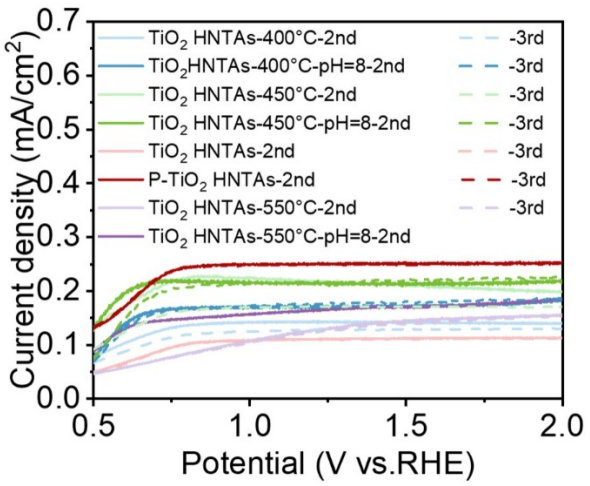

Figure S10. The PEC water oxidation activity (LSV curves) of TiO_2 HNTAs and P-doping TiO_2 HNTAs samples obtained by annealing at different temperatures. [Reaction condition: 0.5 M $NaSO_4$, Xenon lamp (AM 1.5G, 150 mW/cm^2), scan rate 20 mV/s.]

Table S2. The summary of XRD analysis for TiO_2 HNTAs, P-doping TiO_2 HNTAs samples obtained under different calcination temperatures

Catalyst	Annealing temperature	Peak area ratio of (004)/(101)
TiO_2 HNTAs	400 °C	95322/41029=2.32
P-doping TiO_2 HNTAs		165748/21326=7.77
TiO_2 HNTAs	450 °C	199303/66700=2.98
P-doping TiO_2 HNTAs-		264869/34405=7.70
TiO_2 HNTAs-	500 °C	97560/24851=3.92
P-doping TiO_2 HNTAs		231572/30763=7.53
TiO_2 HNTAs-	550 °C	161430/61828=2.61
P-doping TiO_2 HNTAs		132383/37495=3.53

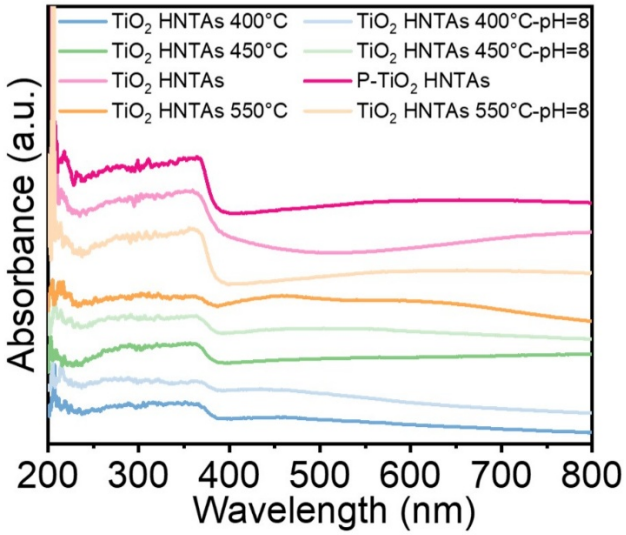

Figure S11. The UV-Vis absorption spectra TiO_2 HNTAs and P-doping TiO_2 HNTAs obtained by annealing at different temperatures.

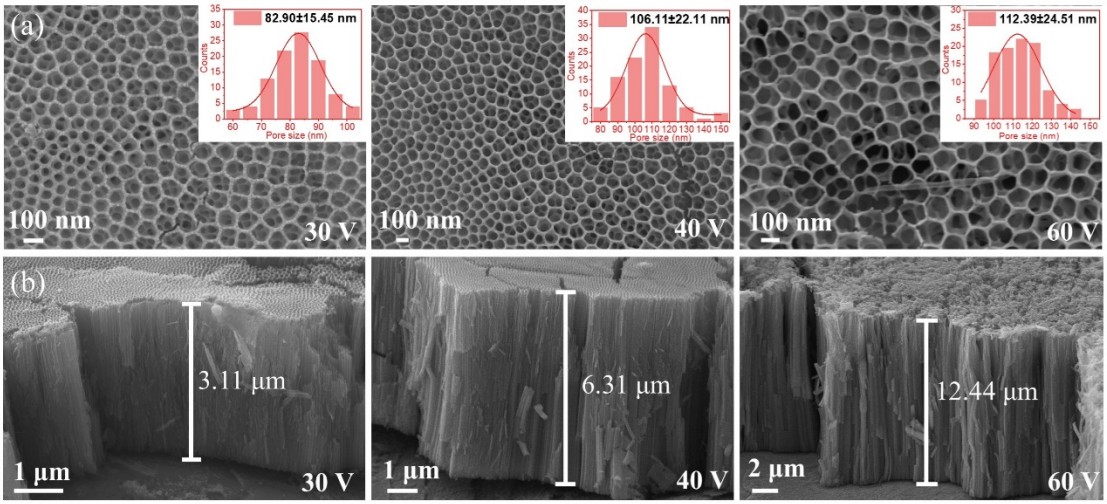

Figure S12 (a) The SEM and pore size distribution and (b) cross-section SEM images for the P-doping TiO_2 HNTAs samples obtained at different anodization voltages (30 V, 40 V and 60 V, the data for 50 V has been provided before).

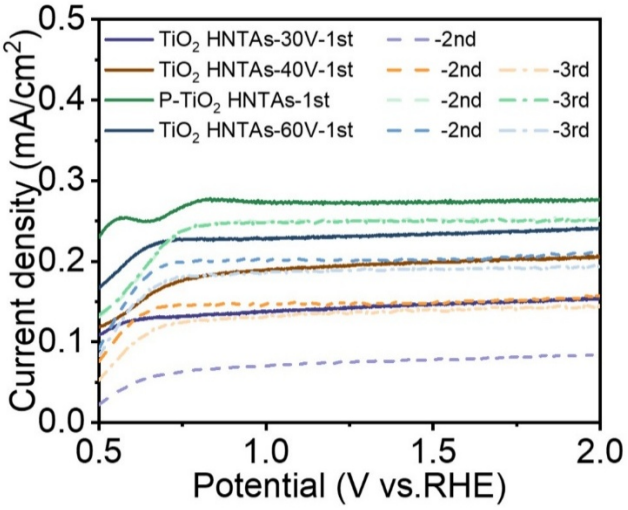

Figure S13. The PEC water oxidation activity (LSV curves) of P-doping TiO_2 HNTAs samples obtained by annealing at different temperatures. [Reaction condition: 0.5 M Na_2SO_4, Xenon lamp (AM 1.5G, 150 mW/cm^2), scan rate 20 mV/s.]

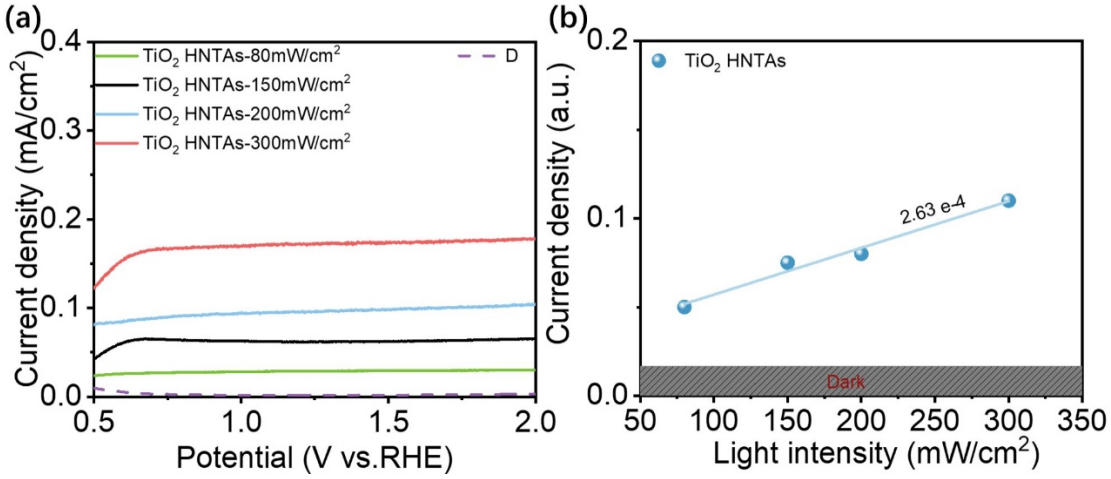

Figure S14. (a) LSV curves of TiO_2 HNTAs under different light intensities and (b) the linear relationship of pure photocurrent density (subtracting the current density in the dark) at 1.23 V vs. RHE with light intensity. [Reaction condition: 0.5 M Na_2SO_4, Xenon lamp (AM 1.5G, 80-300 mW/cm^2), scan rate 20 mV/s.]

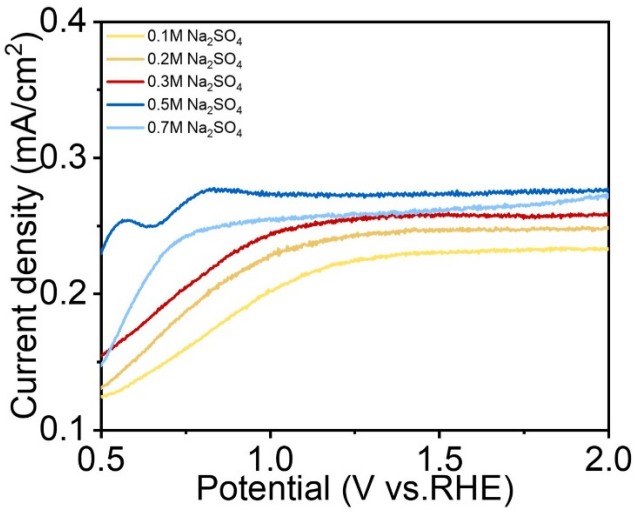

Figure S15. The LSV curves of PEC water oxidation in different concentration of Na_2SO_4 electrolyte with P-TiO_2 HNTAs as catalyst. [Reaction condition: Na_2SO_4, Xenon lamp (AM 1.5G, 150 mW/cm^2), scan rate 20 mV/s.]

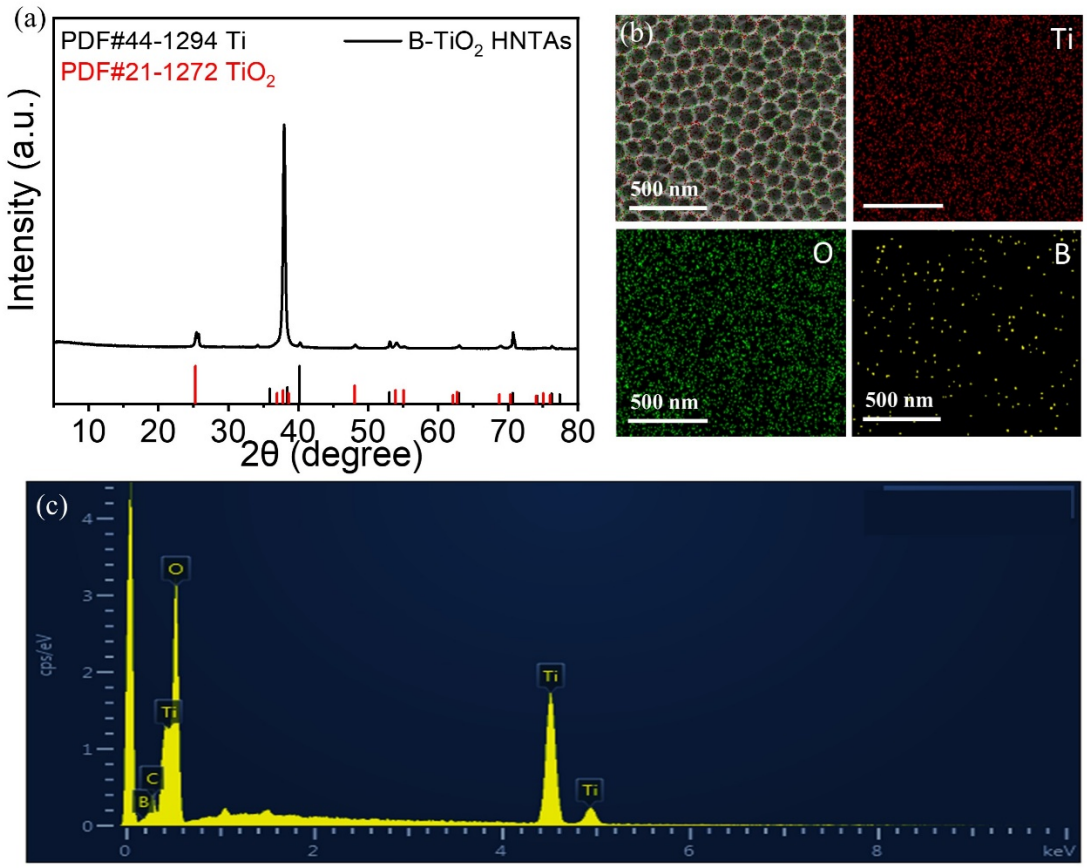

Figure S16. The (a) XRD, (b) SEM and the corresponding EDS elemental mapping as well as the (c) mapping analysis of B-TiO_2 HNTAs.

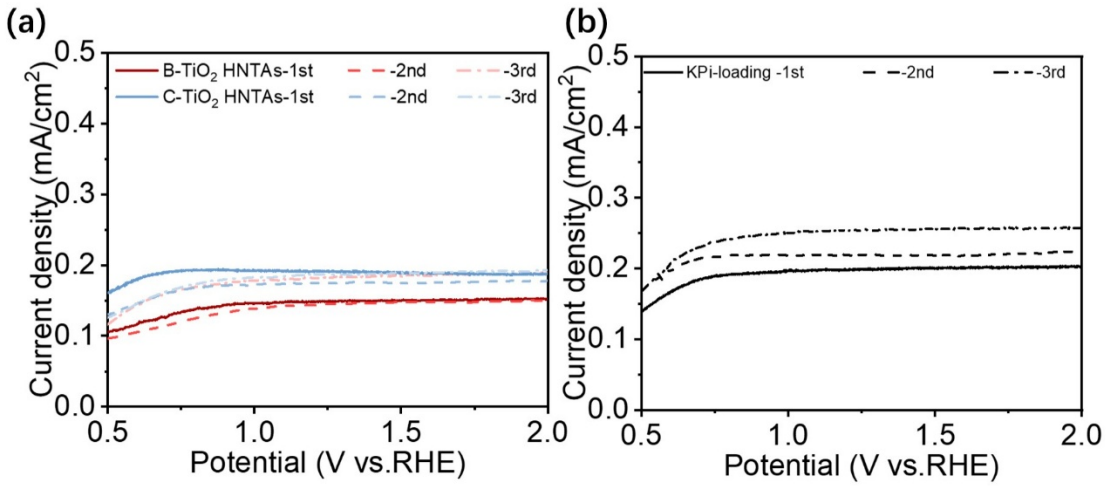

Figure S17. The LSV curves of (a) the samples prepared by using borate and carbonate instead of phosphate and (b) the sample prepared by annealing first followed by dipping in KPi. [Reaction condition: 0.5 M $NaSO_4$, Xenon lamp (AM 1,5G, 150 mW/cm^2), scan rate 20 mV/s.]

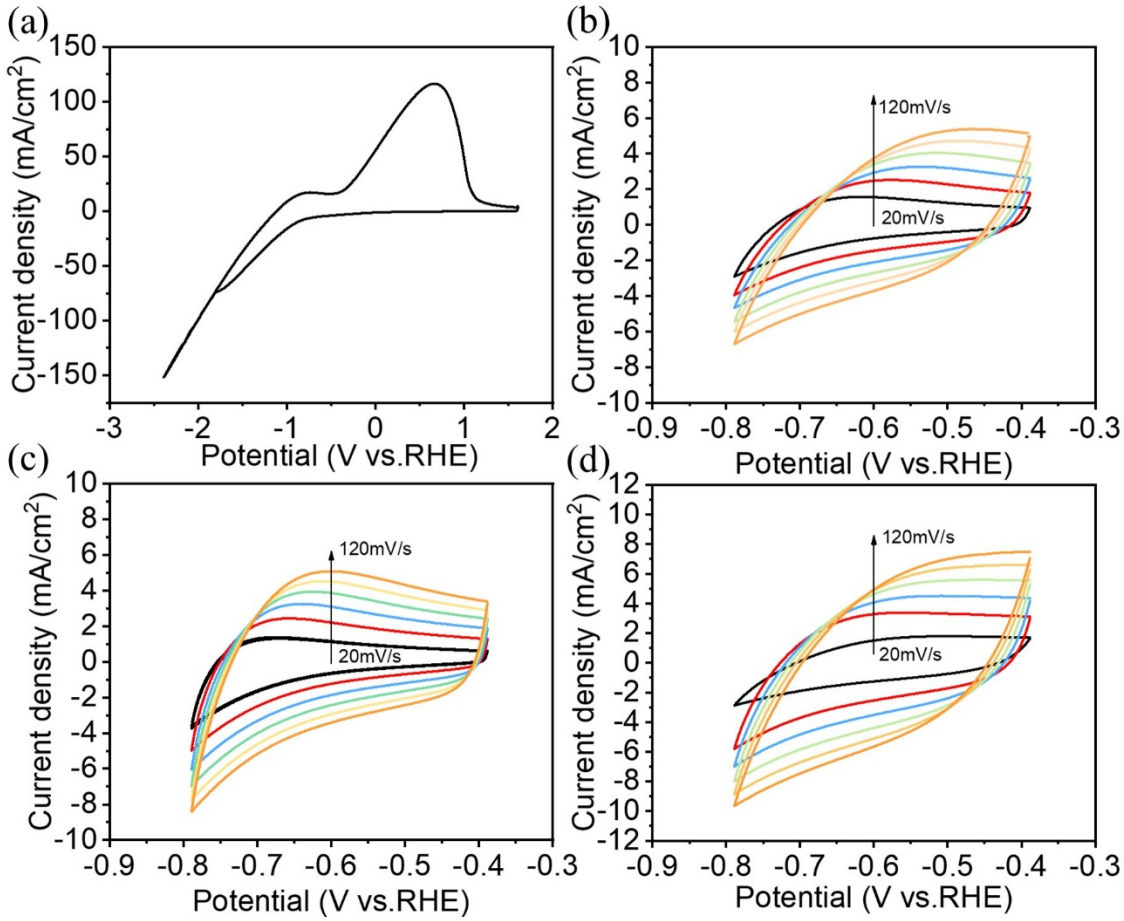

Figure S18. (a) The wide range cyclic voltammetry curve of P-TiO_2 HNTAs tested in 0.5 M $NaSO_4$ with a scan rate of 100 mV/s and the corresponding CV with different scan rates in non-faradaic zone for (b) TiO_2 NTAs, (c) TiO_2 HNTAs and (d) P-TiO_2 HNTAs.

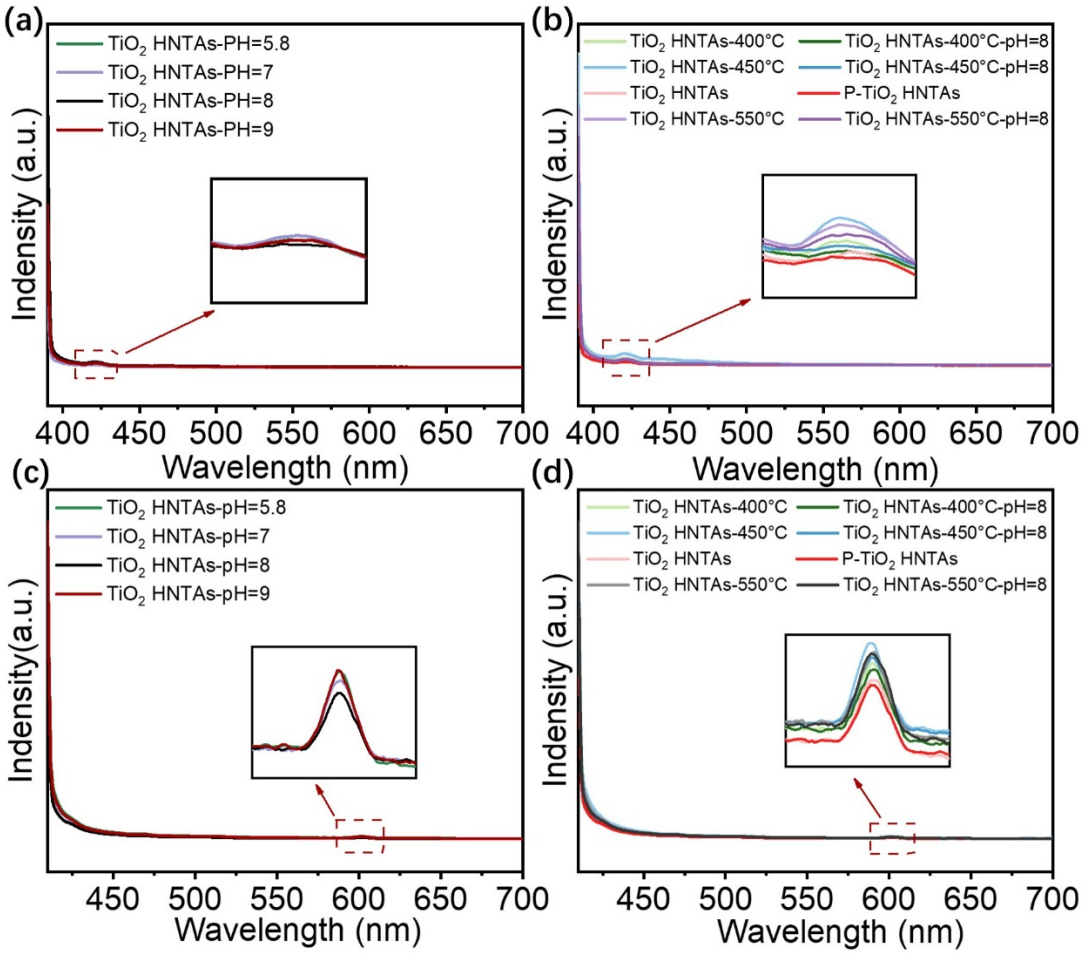

Figure S19. PL of P-TiO_2 HNTAs samples prepared by using (a) different pH of KPi (b) different calcination temperatures. [Excitation wavelength 380 nm]. PL of P-TiO_2 HNTAs samples prepared by using (c) different pH of KPi (d) different calcination temperatures. [Excitation wavelength 400 nm]

.

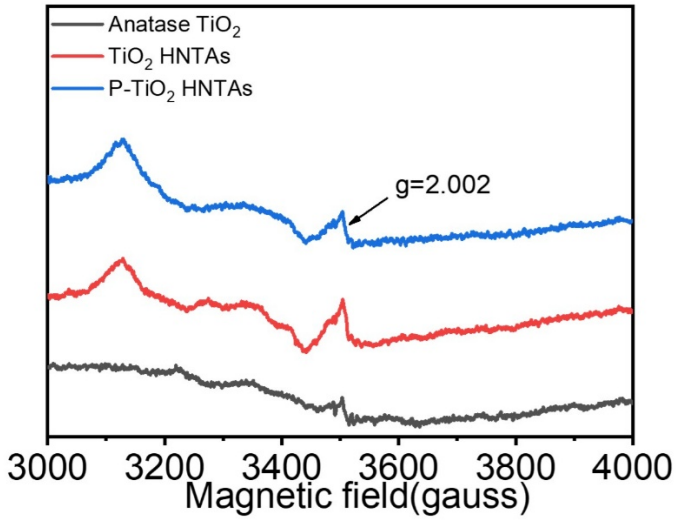

Figure S20. The EPR spectra of commercial anatase-TiO_2, prepared TiO_2 HNTAs and P-TiO_2 HNTAs.

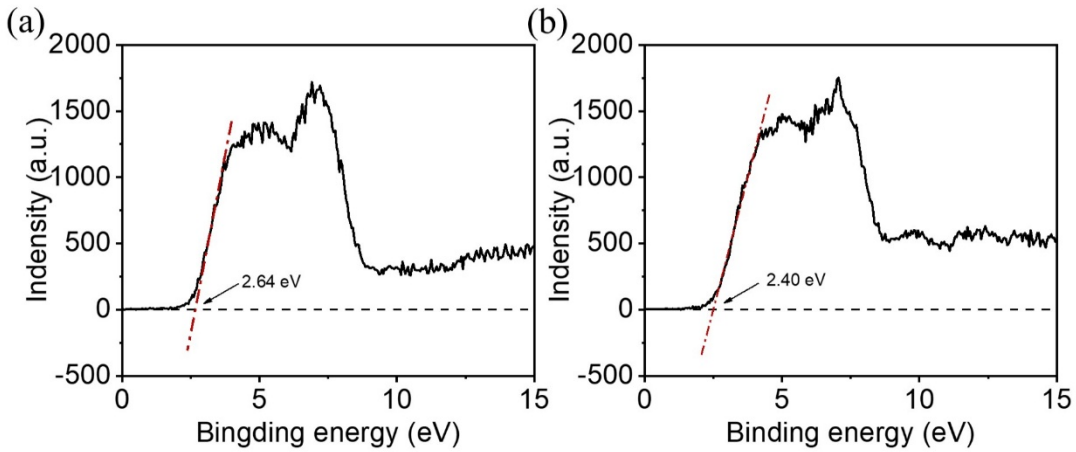

Figure S21. The XPS valence band spectrum of (a) TiO_2 HNTAs and (b) P-TiO_2 HNTAs powder.

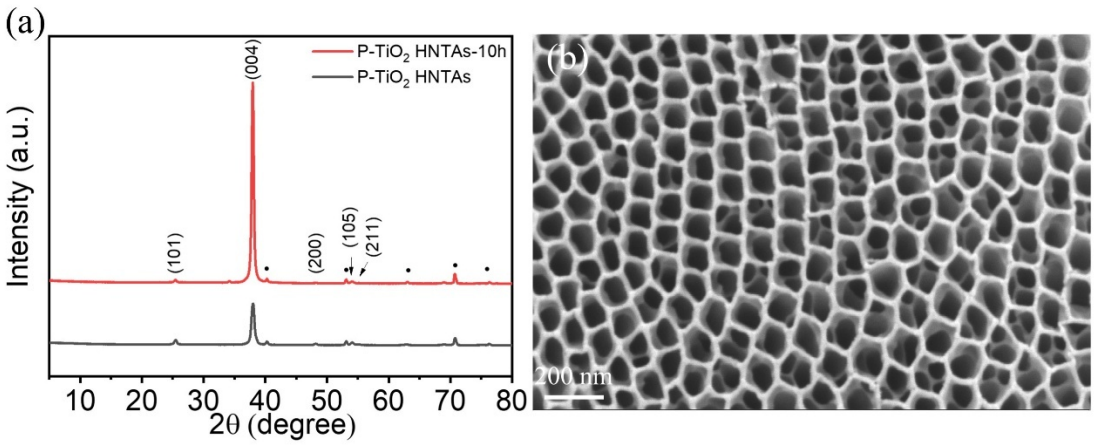

Figure S22. (a) The XRD pattern of the sample, * indicates the peak of the titanium foil substrate and (b) SEM image of P-TiO_2 HNTAs recycled after photostability test for 10 h.

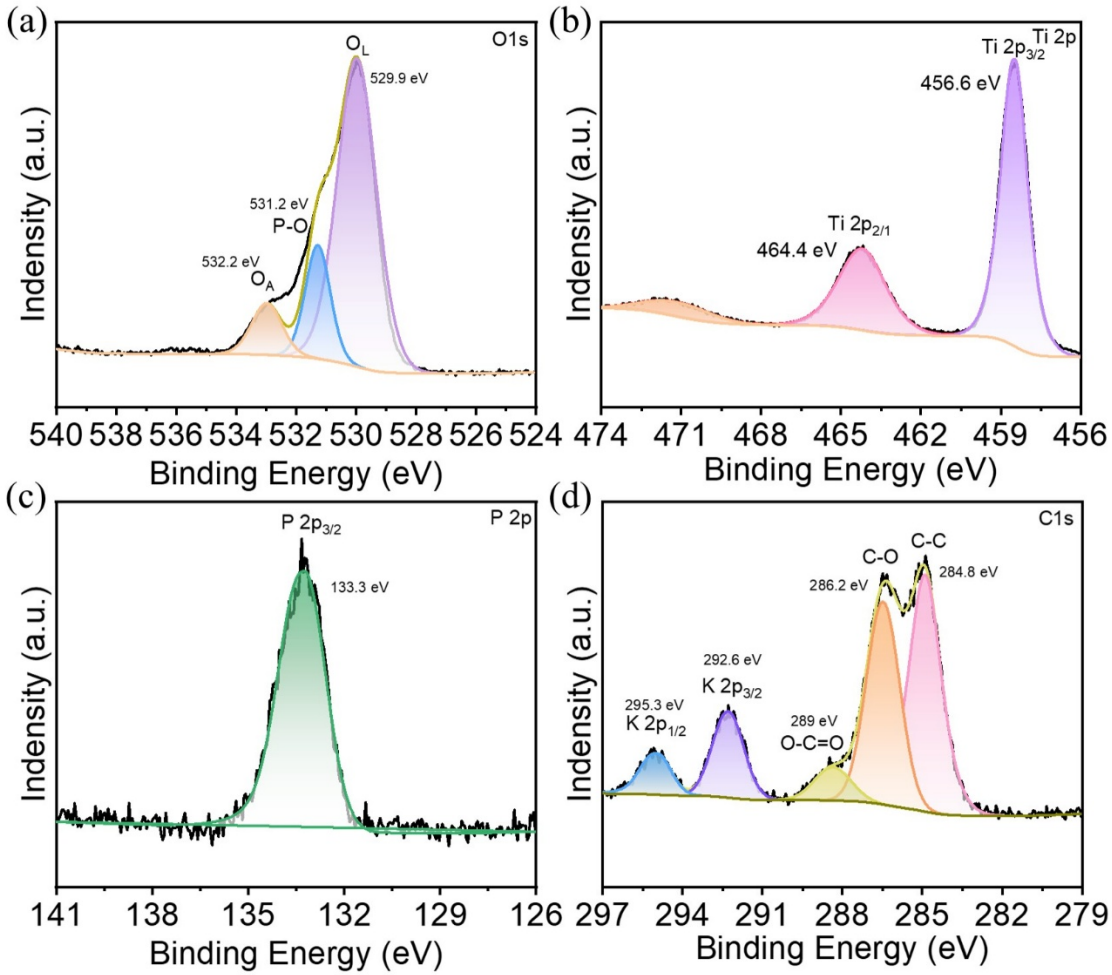

Figure S23. The XPS analysis of P-TiO_2 HNTAs after photostability test for 10 h. (a) O 1s, (b) Ti 2p, (c) P 2p and (d) C 1s.

Table S3. Compared the performance of P-TiO_2 HNTAs with the catalysts reported in literatures on PEC water oxidation.

Catalyst	Wavelength and intensity of light	Electrolyte concentration	The current density at 1.23 V vs. RHE	Ref
P-TiO_2 NTs	λ>420nm,100 mW/cm^2	1.0 M NaOH	0.24 mA/cm^2	1
N-doped TiO_2	λ>420nm,100 mW/cm^2	1.0 M NaOH	0.2 mA/cm^2	2
CoPi/N-TNA	λ=460nm,100 mW/cm^2	0.2 M K_3PO_4	0.1 mA/cm^2	3
FTO/TiO_2/Si/NiO	AM1.5G,100 mW/cm^2	1.0 M KOH	0.65 mA/cm^2	4
CoAl(OH)x/citrate/Sb-TiO_2NRs	AM1.5G,150 mW/cm^2	0.5 M Na_2SO_4	1.78 mA/cm^2	5
α-$SnWO_4$	AM1.5G,100 mW/cm^2	0.1 M KPi	1.9 mA/cm^2	6
3D Fe_2O_3/Ni NC	AM1.5G,100 mW/cm^2	1 M NaOH	1.86 mA/cm^2	7
P-TiO_2 HNTAs	AM1.5G,150 mW/cm^2	0.5 M Na_2SO_4	0.28 mA/cm^2	This work

[1] D.D. Qin, Q.H. Wang, J. Chen, C.H. He, Y. Li, C.H. Wang, J.J. Quan, C.L. Tao and X.Q. Lu, *Sustainable Energy Fuels.*, 2017, **1**, 248–253.

[2] M. Praveen Kumar, R. Jagannathan and S. Ravichandran, *Energy Fuels*, 2020, **34**, 9030–9036.

[3] U. Kang, R. Mizuochi, H. Park and K. Maeda, *Small Struct.*, 2023, **4**, 2200229.

[4] K. Shubham, M. K. Ganesha, H. Hakkeem, A. M. Chandran, A. S. Mary, A. Anand, D. De, D. Sarkar, G. G. Khan and A. K. Singh, *J. Mater. Chem. A*, 2025, **13**, 10844–10854.

[5] D. Pal, D. Maity, D. De, M. K. Ganesha, A. K. Singh, S. Bhaladhare and G. G. Khan, *Int. J. Hydrogen Energy*, 2024, **51**, 52–65.

[6] A. Anand, A. Raj, D. Mondal, D. Maity, M. K. Ganesha, A. K. Singh, D. De and G. G. Khan, *Adv. Funct. Mater.*, 2025, **35**, 2417398.

[7] A. K. Singh and D. Sarkar, *ChemCatChem*, 2019, **11**, 6355–6363.